THE JOURNAL OF BIOLOGICAL CHEMISTRY
Vol. 279, No. 35, Issue of August 27, pp. 36372–36381, 2004

Printed in U.S.A.

Molecular Basis of the Differential Sensitivity of Nematode and Mammalian Muscle to the Anthelmintic Agent Levamisole*

Received for publication, March 19, 2004, and in revised form, May 28, 2004
Published, JBC Papers in Press, June 16, 2004, DOI 10.1074/jbc.M403096200

Diego Rayes, María José De Rosa, Mariana Bartos, and Cecilia Bouzat‡

From the Instituto de Investigaciones Bioquímicas de Bahía Blanca, UNS-CONICET, B-8000FWB Bahía Blanca, Argentina

Levamisole is an anthelmintic agent that exerts its therapeutic effect by acting as a full agonist of the nicotinic receptor (AChR) of nematode muscle. Its action at the mammalian muscle AChR has not been elucidated to date despite its wide use as an anthelmintic in humans and cattle. By single channel and macroscopic current recordings, we investigated the interaction of levamisole with the mammalian muscle AChR. Levamisole activates mammalian AChRs. However, single channel openings are briefer than those activated by acetylcholine (ACh) and do not appear in clusters at high concentrations. The peak current induced by levamisole is about 3% that activated by ACh. Thus, the anthelmintic acts as a weak agonist of the mammalian AChR. Levamisole also produces open channel blockade of the AChR. The apparent affinity for block (190 μM at −70 mV) is similar to that of the nematode AChR, suggesting that differences in channel activation kinetics govern the different sensitivity of nematode and mammalian muscle to anthelmintics. To identify the structural basis of this different sensitivity, we performed mutagenesis targeting residues in the α subunit that differ between vertebrates and nematodes. The replacement of the conserved αGly-153 with the homologous glutamic acid of nematode AChR significantly increases the efficacy of levamisole to activate channels. Channel activity takes place in clusters having two different kinetic modes. The kinetics of the high open probability mode are almost identical when the agonist is ACh or levamisole. It is concluded that αGly-153 is involved in the low efficacy of levamisole to activate mammalian muscle AChRs.

At the neuromuscular junction, acetylcholine (ACh)[1] mediates fast neurotransmission by activating nicotinic receptors (AChRs). AChRs in nematode muscle are targets for anthelmintic chemotherapy. Levamisole and pyrantel are two widely used anthelmintic drugs. By binding to the AChR they lead to a depolarization of the somatic muscle of nematodes. The efficacy of these drugs is based on their ability to act as full agonists of AChRs in nematodes (1). Contractility and membrane potential measurements have shown that the nematode axial muscle is 10–100 times more sensitive to the acute action of pyrantel and levamisole than the rat muscle (2). The molecular bases of this selectivity have not been yet elucidated. The kinetics of activation of nematode AChRs by levamisole has been studied in several preparations from parasite muscle (1, 3), but its action on mammalian muscle AChRs has not been described to date. The effects of levamisole on human neuronal $\alpha_3\beta_2$ and $\alpha_3\beta_4$ AChRs have been studied recently (4) with the voltage clamp method. It was shown that levamisole behaves as a weak partial agonist, an allosteric modulator, and an open channel blocker of neuronal AChRs (4).

ACh is responsible for neuromuscular transmission in nematodes (1). In *Caenorhabditis elegans* muscle, levamisole-activated AChRs are composed of the *unc-38* subunit, which encodes an α subunit, and *lev-1* and *unc-29,* which encode non-α subunits (5). Expression studies in *Xenopus* oocytes have shown that both *unc-38* and *unc-29* subunits are necessary for AChR function (5). Both subunits are required for the expression of levamisole-sensitive receptors in body wall muscles of these nematodes (6). Other nematode α subunits have been cloned from the parasitic nematodes *Trichostrongylus colubriformis* (7), *Haemonchus conturtus* (8), and *Ascaris suum* (9), showing a 91.6, 91, and 76% similarity with *unc-38,* respectively. The main structural features of the AChR subunits are strikingly conserved in phylogeny from higher organisms to the nematode. However, residues differentially conserved between mammalian and nematode AChRs may lead to a differential pharmacological action of anthelmintics at AChRs.

In this study, we explore for the first time the interaction of levamisole with mammalian muscle AChRs at the single channel and macroscopic current levels. Our results reveal that levamisole shows an extremely low efficacy for channel activation. At high levamisole concentrations, channel blockade also contributes to maintain a low probability of channel opening. In contrast, levamisole has been shown to act as a potent agonist of different nematode muscle AChRs (3, 10–12). Thus, this anthelmintic compound therapeutically exploits differences by selectively activating the AChR of the parasite and not that of the host. To identify residues involved in this different selectivity, we combined site-directed mutagenesis at residues differentially conserved between muscle α subunits from nematodes and vertebrates, and we evaluated the changes in levamisole activation. Our results reveal that the glutamic acid at position 153, which is highly conserved in all nematode α subunits cloned to date, may be involved in the potent activation of nematode AChRs by levamisole.

The elucidation of the molecular basis of anthelmintic acti-

* This work was supported by grants from Universidad Nacional del Sur, Agencia Nacional de Promoción Científica y Tecnológica, International Society for Neurochemistry, CONICET (to C. B.), and FIRCA Grant 1R03 TW01185-01 (to C. B. and Steven Sine, Principal Investigator of the FIRCA Grant, Mayo Clinic and Foundation, Rochester, MN). The costs of publication of this article were defrayed in part by the payment of page charges. This article must therefore be hereby marked "*advertisement*" in accordance with 18 U.S.C. Section 1734 solely to indicate this fact.

‡ To whom correspondence should be addressed: Instituto de Investigaciones Bioquímicas de Bahía Blanca, UNS-CONICET, CC857, Camino La Carrindanga Km 7-B8000FWB Bahía Blanca, Argentina. Fax: 54-291-4861200; E-mail: inbouzat@criba.edu.ar.

[1] The abbreviations used are: AChR, nicotinic acetylcholine receptor; ACh, acetylcholine; P_{open}, channel open probability; HEK cells, human embryonic kidney cells.

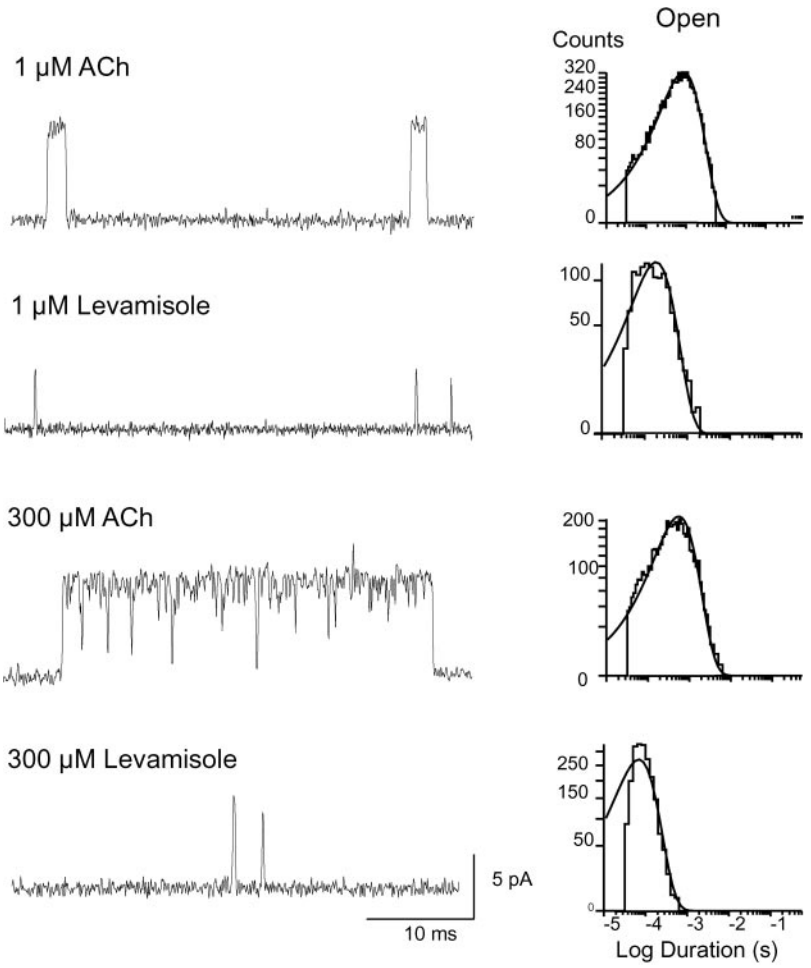

FIG. 1. **Adult mammalian muscle AChRs activated by levamisole.** Channels activated by 1 and 300 μM ACh or levamisole were recorded from HEK cells expressing $\alpha_2\beta\epsilon\delta$ AChRs. *Left,* traces of currents are displaced at a bandwidth of 9 kHz with channel openings as upward deflections. *Right,* open time histograms corresponding to each condition. Membrane potential, −70 mV. The data are representative of 4–8 recordings for each condition.

vation of AChRs will greatly contribute to the development of more selective therapies against parasites and to the understanding of how parasites develop resistance to the anthelmintics. In addition, it pinpoints determinants of function.

EXPERIMENTAL PROCEDURES

Site-directed Mutagenesis and Expression of AChR—HEK293 cells were transfected with mouse α (wild-type or mutant), β, δ, and ϵ cDNAs using calcium phosphate precipitation at a subunit ratio of 2:1:1:1 for α:β:δ:ϵ, respectively, mainly as described previously (13, 14). A plasmid encoding green fluorescent protein (pGreen lantern) was also included for recordings to allow identification of transfected cells under fluorescence optics. Mutant subunits were constructed using the QuikChange™ site-directed mutagenesis kit (Stratagene). Restriction mapping and DNA sequencing confirmed all constructs. Cells were used for patch clamp recordings 48 h after transfection.

Patch Clamp Recordings and Kinetic Analysis—Recordings were obtained in the cell-attached configuration (15) at 20 °C (13). The bath and pipette solutions contained 142 mM KCl, 5.4 mM NaCl, 1.8 mM $CaCl_2$, 1.7 mM $MgCl_2$, and 10 mM HEPES (pH 7.4). Acetylcholine (ACh), levamisole (Sigma), or both drugs were added to the pipette solution. Single channel currents were recorded using an Axopatch 200 B patch clamp amplifier (Axon Instruments, Inc., CA), digitized at 5-μs intervals with the PCI-611E interface (National Instruments, Austin, TX), recorded to the hard disk of a computer using the program Acquire (Bruxton Corporation, Seattle, WA), and detected by the half-amplitude threshold criterion using the program TAC 4.0.10 (Bruxton Corporation, Seattle, WA) at a final bandwidth of 10 kHz. Open and closed time histograms were plotted using a logarithmic abscissa and a square root ordinate and fitted to the sum of exponentials by maximum likelihood using the program TACFit (Bruxton Corp., Seattle, WA).

Clusters were identified as a series of closely spaced events preceded and followed by closed intervals longer than a specified duration (t_{crit}); this duration was taken as the point of intersection of the predominant closed time component and the succeeding one in the closed time histogram. Clusters showing double openings were discarded. For each recording, clusters were selected on the basis of their distribution of open probability (P_{open}), mean open duration, and mean closed duration (16–18). P_{open} distributions of the αG153E mutant AChR show two clear components, which were defined as high P_{open} (HP_{open}) and low P_{open} (LP_{open}) mode. Clusters of each mode were first selected to allow a separate kinetic analysis for each mode. For the analysis, we only used clusters that showed only one gating mode. For the high P_{open} mode activated by ACh and levamisole, the kinetic analysis was restricted to clusters, each reflecting the activity of a single AChR (16–18). The resulting open and closed intervals from the selected clusters were analyzed according to kinetic schemes using an interval-based full-likelihood algorithm (www.qub.buffalo.edu) (QuB suite, State University of New York, Buffalo). The dead time was typically 30 μs. Probability density functions of open and closed durations were calculated from the fitted rate constants and instrumentation dead time and superimposed on the experimental dwell time histogram as described by Qin *et al.* (19). Calculated rates were accepted only if the resulting probability density functions correctly fitted the experimental open and closed duration histograms.

The other approach was applied to the low P_{open} gating mode of the αG153E AChR and to wild-type AChRs activated by levamisole, in which less clear or no clusters were observed. We analyzed the behavior of bursts of single channel activity elicited by low agonist concentrations, where no clusters can be seen and block is insignificant, on the basis of the classical activation Scheme 1,

$$RT \underset{k_{-1}}{\overset{k_{+1}}{\rightleftharpoons}} AR \underset{k_{-2}}{\overset{k_{+2}}{\rightleftharpoons}} A_2R \underset{\alpha}{\overset{\beta}{\rightleftharpoons}} A_2R^*$$

SCHEME 1

where two agonists (A) bind to the receptor (R) in the resting state with association rates k_{+1} and k_{+2} and dissociate with rates k_{-1} and k_{-2}. AChRs occupied by two agonist molecules open with rate β and close with rate α. Bursts at low agonist concentrations contain information

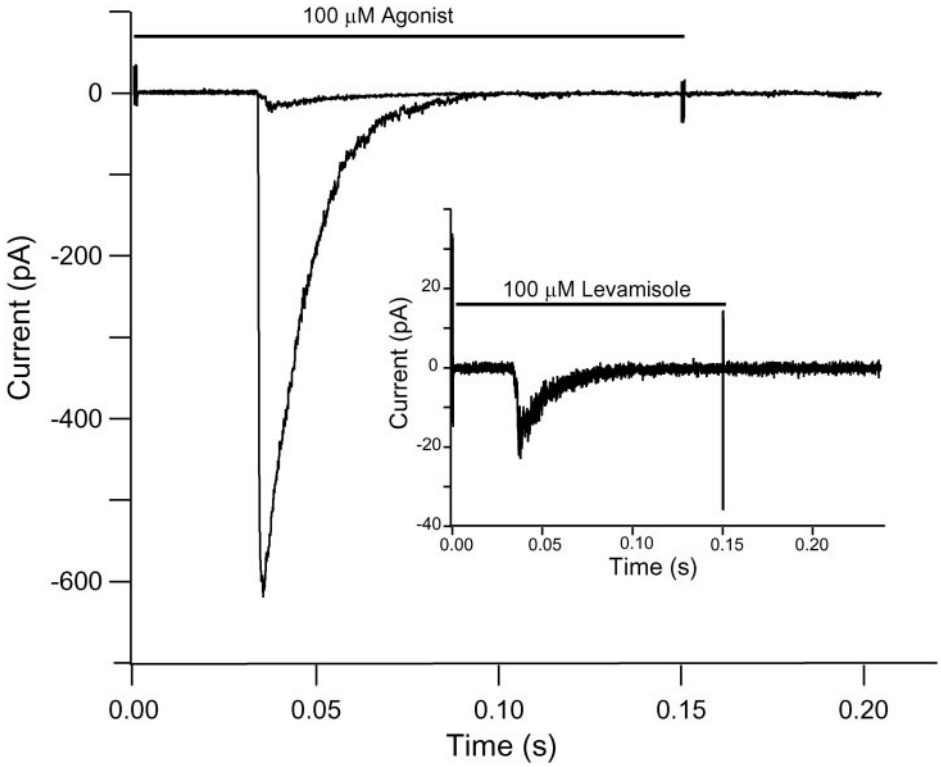

FIG. 2. **Macroscopic currents activated by 100 μM ACh or levamisole.** Currents recorded from an outside-out patch in response to rapid perfusion of 100 μM ACh and 100 μM levamisole. The *solid bar* indicates the duration of the exposure to agonist. The levamisole current is shown alone at a different scale. Each *trace* represents the average of 6–10 applications of agonist or extracellular solution. Membrane potential, −50 mV.

about the open state and the immediately adjacent closed state (16). Therefore, estimates of β, α, and k_{-2} can be obtained from the mean duration of the briefer component of the closed time histogram (τ_c), its relative area ($A\tau_c$), and the mean burst duration (τ_b) as follows: $\tau_c = 1/(\beta + k_{-2})$; $A\tau_c = \beta/(\beta + k_{-2})$; $\tau_b = (1 + \beta/k_{-2})\ (1/\alpha)$.

Macroscopic Current Recordings—For outside-out patch recordings, the pipette solution contained 140 mM KCl, 5 mM EGTA, 5 mM $MgCl_2$, and 10 mM HEPES (pH 7.3). Extracellular solution contained 150 mM NaCl, 5.6 mM KCl, 1.8 mM $CaCl_2$, 1 mM $MgCl_2$, and 10 mM HEPES (pH 7.3). The patch was excised in this configuration and moved into position at the outflow of a perfusion system as described before (20, 21). The perfusion system allows for a rapid (0.1–1 ms) exchange of the solution bathing the patch. A series of applications of extracellular solution containing ACh, levamisole, or both drugs were applied to the patch during 150 ms. Macroscopic currents were filtered at 5 kHz, digitized at 20 kHz, and stored on the hard disk. Data analysis was performed using the IgorPro software (WaveMetrics Inc., Lake Oswego, OR). The ensemble mean current was calculated for 5–10 individual current traces. Mean currents were usually fitted by a single exponential function: $I_{(t)} = I_0 \exp(-t/\tau_d) + I_\infty$ where I_0 and I_∞ are the peak and the steady state current values, respectively, and τ_d is the decay time constant that measures the current decay due to desensitization. Current records were aligned with each other at the point where the current reached 50% of its maximum level.

RESULTS

Activation of Mammalian AChRs by Levamisole

Single Channel Currents Activated by Levamisole—Levamisole is a full agonist of the nematode muscle AChR (1). In the present study, we evaluated if this anthelmintic drug also acts on mammalian muscle AChRs. To this end, we first recorded single channels from cells expressing adult muscle AChRs (Fig. 1). As shown in this figure, levamisole is capable of activating mammalian AChRs. However, channel openings are significantly briefer than those activated by the endogenous neurotransmitter ACh. Open time distributions of 1 μM levamisole-activated AChRs can be well fitted by a main component of 220 ± 20 μs (relative area >0.7) (Fig. 1). The duration of the main open component is 4-fold briefer than that observed at 1 μM ACh (860 ± 80 μs, Fig. 1) (13, 14).

Increasing levamisole concentration from 1 to 300 μM does not produce the typical clustering observed with full agonists, such as ACh. At ACh concentrations higher than 10 μM, wild-type AChRs open in clusters of well defined activation episodes (17) (Fig. 1). Each activation episode begins with the transition of a single receptor from the desensitized to the activable state and terminates by returning to the desensitized state. At 300 μM ACh, the probability of channel opening within a cluster is ~1 (17; Fig. 1). In contrast, when AChRs are activated by levamisole, even at concentrations as high as 300 μM, clusters are not observed (Fig. 1). These results suggest that levamisole opens mammalian AChRs with greater latency and closes them faster than ACh.

Increasing levamisole concentration from 1 to 300 μM leads to a significant reduction of open durations. Open time histograms of AChRs activated by 300 μM levamisole can be fitted by a single exponential with a mean open time of 80 ± 9 μs (Fig. 1). Such a concentration-dependent decrease in the mean open time indicates that in addition to its capability of activating mammalian AChRs, levamisole may act as an open channel blocker (see below).

Macroscopic Currents Activated by Levamisole—To evaluate the efficacy of levamisole in activating mammalian AChRs, we recorded macroscopic currents from outside-out patches rapidly perfused with levamisole. Fig. 2 shows ensemble currents obtained from a single outside-out patch exposed to brief applications of 100 μM ACh (control) and 100 μM levamisole. In control data, the current reaches the peak after 0.1–1 ms and then decays with a time constant (τ_d) of about 20–30 ms due to desensitization (Fig. 2) (20). The peak current is only about 3% when the same patch is exposed to 100 μM levamisole. Moreover, in many patches only single channels were observed after perfusion with levamisole. These results confirm the low efficacy of the drug to activate mammalian AChRs.

Open Channel Blockade of AChRs by Levamisole

Given that the single channel recording experiments suggest that levamisole may also block AChRs (Fig. 1), we studied its action as a channel blocker in the absence and presence of ACh. Increasing levamisole concentration systematically displaces

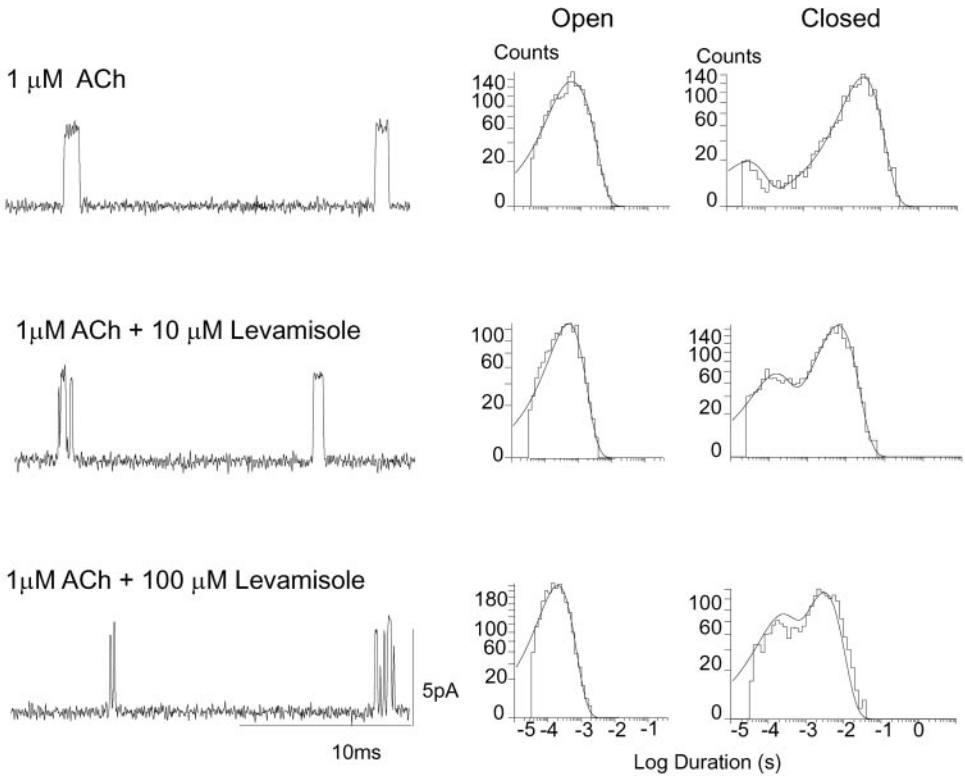

FIG. 3. **Combined action of ACh and levamisole on mammalian AChRs.** *Left,* traces of currents recorded in the presence of 1 μM ACh and 10 or 100 μM levamisole. Currents are displaced at a bandwidth of 9 kHz with channel openings as upward deflections. Membrane potential, −70 mV. *Right,* closed and open time histograms of the corresponding recordings. The data are representative of 3–5 recordings for each condition.

to briefer durations the open time distributions of AChR channels activated either by 1 μM ACh (Fig. 3) or by levamisole (Fig. 1).

We used the classical linear blocking model to describe the action of levamisole as an open channel blocker as shown in Scheme 2,

$$C \underset{\alpha}{\overset{\beta}{\longleftrightarrow}} O \underset{k_{-b}}{\overset{k_{+b}[B]}{\longleftrightarrow}} OB$$

SCHEME 2

where C indicates closed, O indicates open, and OB indicates blocked states. In agreement with Scheme 2, a linear relationship between the reciprocal of the mean open time and levamisole concentration ($[B]$) is observed (Fig. 4*a*). The calculated value for the forward rate constant of the blocking reaction (k_{+b} in Scheme 2), given by the slope of the curve, is 30×10^6 and 25×10^6 M^{-1} s^{-1} for ACh- or levamisole-activated channels. Thus, AChRs activated by either ACh or levamisole are blocked by levamisole at a similar rate. The apparent closing rate, calculated from the intercept with the y axis, is 5600 s^{-1} for levamisole-activated AChRs and 1600 s^{-1} for ACh-activated channels. This value agrees with the closing rate of ACh-activated channels calculated by kinetic analysis (17, 18).

To analyze the blockade by levamisole, we studied the closed time distributions of AChRs activated by 1 μM ACh in the presence of levamisole. In its absence, closed time histograms corresponding to 1 μM ACh-activated channels show a main component whose duration is dependent on the number of channels in the patch (17) (Fig. 3). The presence of levamisole significantly changes the closed time distributions of ACh-activated channels, and a new closed component of about 175 μs is systematically observed (Fig. 3). The duration of this component does not change with levamisole concentration, but its area increases as a function of its concentration (Fig. 4*b*). It is therefore possible to assume that this closed component corresponds to the blockade by levamisole of the ACh-activated channels ($1/k_{-b}$ in Scheme 2). From the duration of this closed component ($1/k_{-b}$) a value of 5700 s^{-1} is obtained for k_{-b}. Thus, the apparent dissociation constant for the blocking process, $K_B = k_{-b}/k_{+b}$, is 190 μM at a membrane potential of −70 mV.

At levamisole concentrations higher than 100 μM, the blocked area does not increase as a function of concentration. The values for the closed components and relative areas are 175 ± 12 μs and 0.32 ± 0.03, and 220 ± 15, and 0.33 ± 0.08 μs for 100 and 300 μM levamisole, respectively. Therefore, at higher concentrations the channel block mechanism deviates from Scheme 2.

The duration of the blocked periods increases with higher negative membrane potentials, indicating that the unblocking process is voltage-dependent (Fig. 4*c*). The voltage dependence of the effect is confirmed by outside-out patch recordings (Fig. 4*d*). At positive membrane potentials, 100 μM levamisole does not affect the decay constant of currents elicited by 1 mM ACh, and the data can be fitted by a single exponential decay similar to the control (22.5 ms). In contrast, at −70 mV, an initial fast decay precedes desensitization. This fast component (about 0.5 ms) is due to open channel blockade. The slow decay time constant, which corresponds to desensitization, is 19.4 ± 1.8 ms. The peak current is not affected, suggesting that at the ratio of concentrations that are used, levamisole cannot compete with ACh for channel activation. In short, the characterization of the blockade indicates that levamisole acts as a typical open channel blocker at concentrations below 100 μM.

Structural Basis of the Weak Activation of Mammalian AChRs by Levamisole

Sequence comparison reveals key residues that are differentially conserved between mammalian and nematode muscle α subunits (Fig. 5). To identify if these residues are involved in

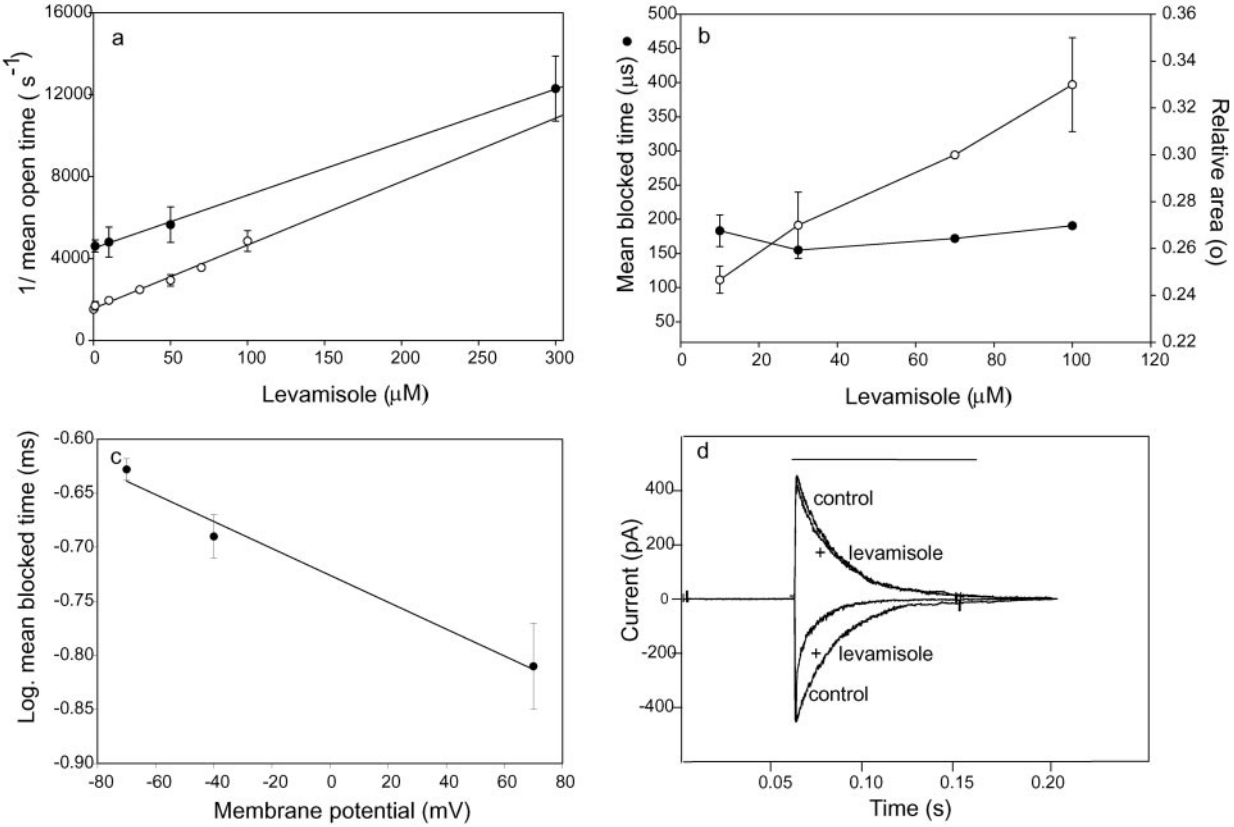

FIG. 4. **Characterization of levamisole blockade.** *a*, AChR channels were recorded in the absence (●) and presence (○) of 1 μM ACh plus levamisole at different final concentrations. The mean open times were obtained from the corresponding open time histograms. The data are fitted by the equation 1/mean open time = $\alpha + k_{+b}$ [levamisole], where k_{+b} is the association rate of levamisole for channel block, and α is the apparent channel closing rate. Data are shown as mean ± S.D. of 3–5 patches. *b*, AChR currents were recorded in the presence of 1 μM ACh plus levamisole. The mean blocked time (●) and its relative area (○) were obtained from the corresponding closed time histograms. Data are shown as mean ± S.D. of 3–5 different recordings for each condition. Membrane potential, −70 mV. *c*, relationship between the mean blocked time and membrane potential. Levamisole concentration, 50 μM. Data are shown as mean ± S.D. of 3–5 patches. *d*, rapid perfusion currents activated by 1 mM ACh (*control*) alone and together with 100 μM levamisole (+ *levamisole*). Currents were recorded at −70 mV (downward currents) and +70 mV (upward currents). Each current represents the average of 5–10 records.

							152	**153**	**154**								**190**						
α1 Rat	L	G	T	W	T	Y	**D**	**G**	**S**	V	V	A	H	W	V	F	Y	-	S	C	C	P	N	T
α1 Mouse	L	G	T	W	T	Y	**D**	**G**	**S**	V	V	A	H	W	V	F	Y	-	S	C	C	P	T	T
α1 Human	L	G	T	W	T	Y	**D**	**G**	**S**	V	V	A	H	S	V	T	Y	-	S	C	C	P	D	T
α1 *T.californica*	L	G	I	W	T	Y	**D**	**G**	**T**	K	V	S	H	W	V	Y	Y	-	T	C	C	P	D	T
TAR1 *T.colubriformis*	F	G	S	W	T	Y	**S**	**E**	**N**	L	L	N	R	S	K	N	Y	**P**	S	C	C	P	Q	S
α1 *A.suum*	F	G	S	W	T	Y	**S**	**E**	**D**	L	L	V	R	T	K	N	Y	**P**	S	C	C	P	Q	S
Unc-38	F	G	S	W	T	F	**S**	**E**	**N**	L	L	S	R	A	K	N	Y	**P**	S	C	C	P	Q	S

FIG. 5. **Sequence alignment of muscle α subunits from vertebrate and nematodes.** The sequences were aligned with ClustalW (1.81).

the differential behavior of anthelmintic drugs at parasite and mammalian muscle, we replaced them by the equivalent residues in nematodes, cotransfected cells with the mutant α and wild-type non-α subunits, and we evaluated channel activity elicited by levamisole. The efficacy of levamisole to activate mammalian AChRs is greatly increased when the residue αGly-153 is replaced by a glutamic acid. As shown in Fig. 6, channel activity appears now in easily recognizable clusters at 50 μM levamisole. In contrast, no changes are observed in the activation by levamisole (1–100 μM) of AChRs carrying either the mutations αD152S, αS154N, or the insertion of a proline after αTyr-190 (α191insP).

Clusters of αG153E AChR can be identified at concentrations higher than 10 μM. The clustering of opening events is accompanied by important changes in the closed time histograms. The main component of the closed time distributions, which corresponds to closings within clusters, is displaced to briefer durations as a function of levamisole concentration (Fig. 7).

To uncover the mechanistic consequences of the presence of a glutamic acid at α153, we recorded channels activated by a range of levamisole concentrations (0.1 nM to 300 μM) and analyzed the activity of single channel openings in clusters. In parallel, we compared the kinetics of activation by the full agonist ACh.

When examined in detail, it can be observed that clusters of αG153E activated by either ACh or levamisole are not homogeneous, indicating that this mutant receptor activates in distinct kinetic modes (Fig. 8). The distribution of P_{open} values showed two different components (see "Experimental Procedures"). We therefore classified the clusters as belonging to two main gating modes: an HP_{open} and an LP_{open} mode. At all agonist concentrations, the HP_{open} mode consisted of openings that were significantly longer and closings within clusters that were briefer than those of the LP_{open} mode (Table I). Based on

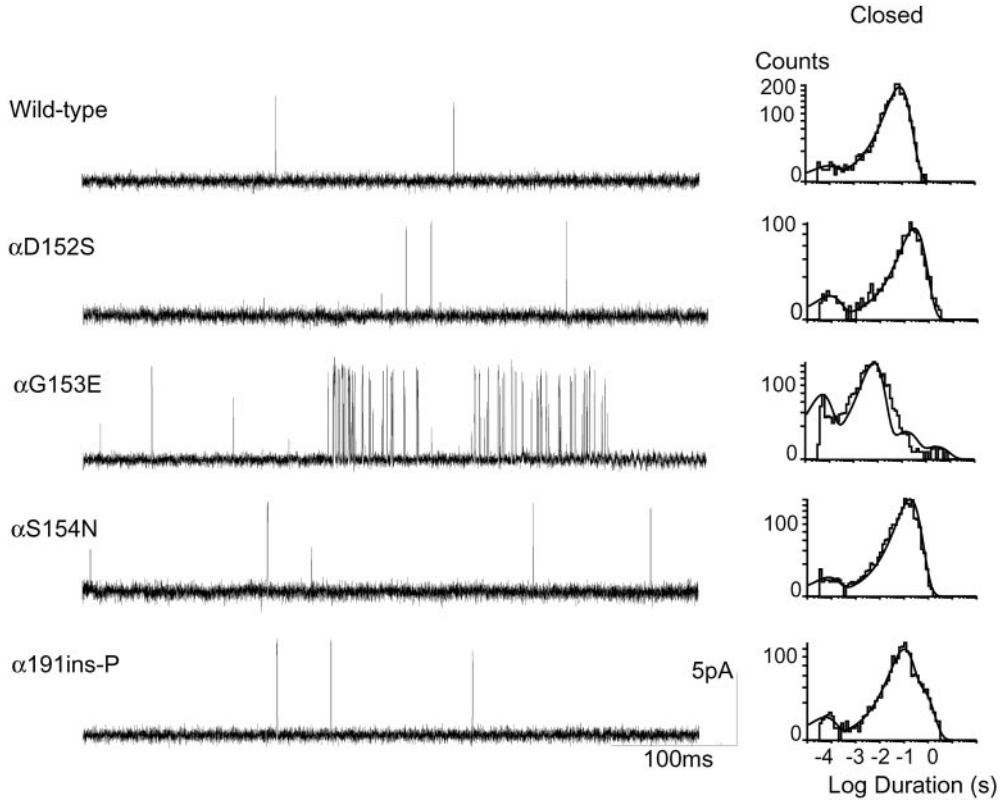

FIG. 6. **Activation of mutant AChRs by levamisole.** Channels activated by 50 μM levamisole were recorded from HEK cells expressing AChRs containing wild-type and the mutant αD152S, αG153E, αS154N, and α191insP subunits. *Left*, currents are displayed at a bandwidth of 9 kHz with channel openings as upward deflections. Membrane potential, −70 mV. *Right*, closed time histograms of AChRs carrying the specified mutant subunit. The data are representative of 4–6 recordings for each condition.

the P_{open} distributions, we selected the clusters corresponding to each mode and analyzed them as a function of agonist concentration (Table I and Fig. 8).

High P_{open} Clusters—At very low concentrations of ACh or levamisole (0.1 nM to1 μM), only clusters corresponding to the high P_{open} gating mode can be observed (Fig. 8). The rest of the openings appear as isolated events. The P_{open} calculated for these clusters is about 1 at 1 nM of either agonist. Most interestingly, there are no significant differences in the properties between ACh- or levamisole-activated clusters (Fig. 8 and Table I). Therefore, at low agonist concentrations, levamisole activation of the αG153E AChR seems to be kinetically indistinguishable from ACh activation. Clusters of the HP_{open} mode are also observed at higher concentrations of both agonists. However, the mean channel duration as well as the P_{open} decrease at higher concentrations of levamisole due to channel blockade (Table I).

Low P_{open} Clusters—As the agonist concentration is increased, clusters of the LP_{open} gating mode can be distinguished (Fig. 8). In contrast to what we observed for the high P_{open} clusters, the low P_{open} ones show marked differences between ACh and levamisole (Table I and Fig. 8). In the presence of ACh, low P_{open} clusters are clearly identified at concentrations higher than 10 μM. The P_{open} of these clusters increases as a function of ACh and reaches a value of about 0.9 at 100 μM ACh (Table I). In addition, the mean open channel duration remains constant, and the mean closed duration within clusters decreases as ACh concentration is increased, indicating that they correspond to agonist-sensitive activation episodes. When levamisole is used as an agonist, low P_{open} clusters can be identified also at concentrations higher than 10 μM. The closed durations separating openings within these clusters decrease as a function of levamisole, as observed for ACh (Table I). However, due to the open channel blockade, the mean open duration and the P_{open} decrease as the concentration is increased. The P_{open} values of the low P_{open} clusters are significantly lower for levamisole than for ACh-activated AChRs (Table I).

To determine the total contribution of the HP_{open} mode to levamisole activation, we thoroughly examined clusters and quantified the proportion of activation episodes corresponding to this mode. Mode switches occur either between clusters or during the course of a single cluster. For example, at 10 μM levamisole, 22 ± 8% of the clusters corresponded to the HP_{open} mode, and 44.22 ± 14.4% of all clusters showed at least one HP_{open} activation episode. Therefore, activation of AChRs in the HP_{open} mode may significantly contribute to the selective action of anthelmintics on nematode AChRs. No channel activity from transfected cells was observed in the absence of agonist in the pipette solution, indicating that neither mode results from spontaneous AChR activation.

Kinetics of Activation of Wild-type and αG153E AChRs by Levamisole

Results from the burst analysis of wild-type AChRs activated by levamisole show a profound decrease in the opening rate (β in Scheme 1) and a 470-fold decrease in the gating equilibrium constant (θ), calculated as β/α, compared with wild-type AChRs activated by ACh (Table II). Thus, the resulting analysis establishes that levamisole is a weak agonist of the AChR mainly due to a very low efficacy for activation. The estimated rates also show that the gating equilibrium constant for the low P_{open} mode of αG153E activated by levamisole is 7-fold higher than that of wild-type AChRs (Table II).

For the HP_{open} gating mode, we selected clusters for both

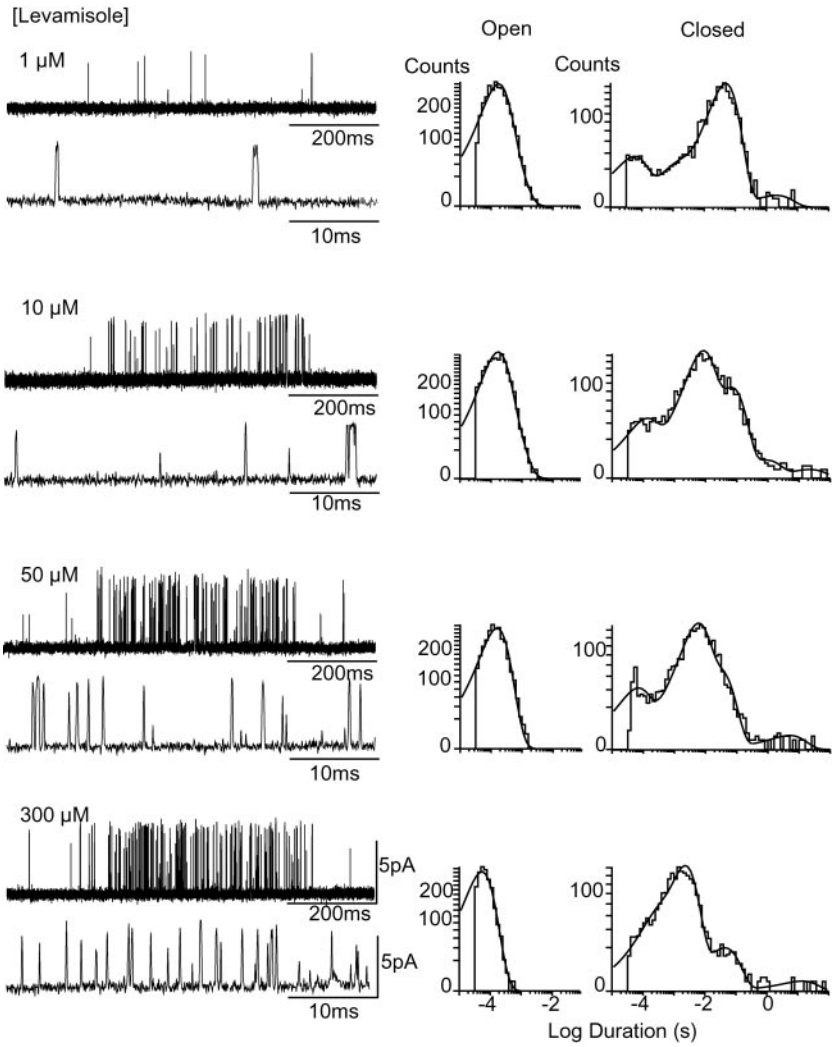

FIG. 7. **Single channel recordings of αG153E mutant AChRs activated by levamisole.** *Left*, channel traces corresponding to AChRs containing the αG153E subunit. Traces are shown at two different time scales for each concentration. Membrane potential, −70 mV. Openings are shown as upward deflections at a bandwidth of 9 kHz. *Right*, open and closed time histograms of the corresponding recordings. The data are representative of 3–7 recordings for each condition.

ACh- and levamisole-activated channels, and we fitted kinetic schemes to the open and closed dwell time histograms of these clusters. In this analysis, it is assumed that an individual cluster originates from the activation of a single ion channel. Given that open and closed time histograms of the HP_{open} population of both ACh- and levamisole-activated AChRs show only one component, we fitted the data to the simplest activation scheme,

$$C \underset{\alpha}{\overset{\beta}{\rightleftharpoons}} O$$

SCHEME 3

where *C* indicates closed and *O* indicates open states of the AChR. The intracluster closed component is constant for all ACh concentrations tested as well as for levamisole concentrations lower than 10 nM, where open blockade is not significant (Table I). We therefore used the data obtained at concentrations of ACh and levamisole lower than 1 μM and 10 nM, respectively. Based on this scheme, the kinetic analysis yielded estimates for the rate constants describing the activation process for both ACh and levamisole. Probability density functions computed from the fitted rate constants superimposed upon open and closed time histograms, showing that activation is adequately described by the scheme. The estimated rate constants are similar for ACh- and levamisole-activated AChRs (Table II). It can therefore be concluded that αG153E shows a gating mode which is highly sensitive to the agonist and is similarly activated by levamisole and ACh.

Position 153 has been detected previously in a slow channel congenital myasthenic patient (αG153S; see Ref. 22). We studied the activation of this mutant AChR by 50 μM levamisole and compared it with that of αG153E. At 50 μM levamisole, single channel recordings show clusters of openings, indicating that levamisole is more efficient to activate αG153S than wild-type AChRs. However, there are some interesting differences with respect to levamisole activation of αG153E. 1) No high P_{open} clusters are observed when αG153S is activated by 50 μM levamisole. Recordings contain only homogeneous clusters with a mean open channel duration of 0.14 ± 0.01 ms, a mean closed time of 10.00 ± 0.65 ms, and a P_{open} of 0.013 ± 0.003. These values are similar to those of LP_{open} clusters of the αG153E AChR at the same agonist concentration (Table I). 2) Well defined clusters of the αG153S occur at levamisole concentrations higher than 30 μM, but the threshold for forming clusters is 10 μM for αG153E AChRs. Therefore, it seems likely that both the position and the type of amino acid are important in making AChRs highly sensitive to anthelmintics.

DISCUSSION

Levamisole contracts the cut-worm preparation in *C. elegans*, depolarizes and produces spastic paralysis of *A. suum* muscle cells, and activates strongly all nematode muscle AChRs (3, 10, 23). Measurements of muscle contractility and membrane

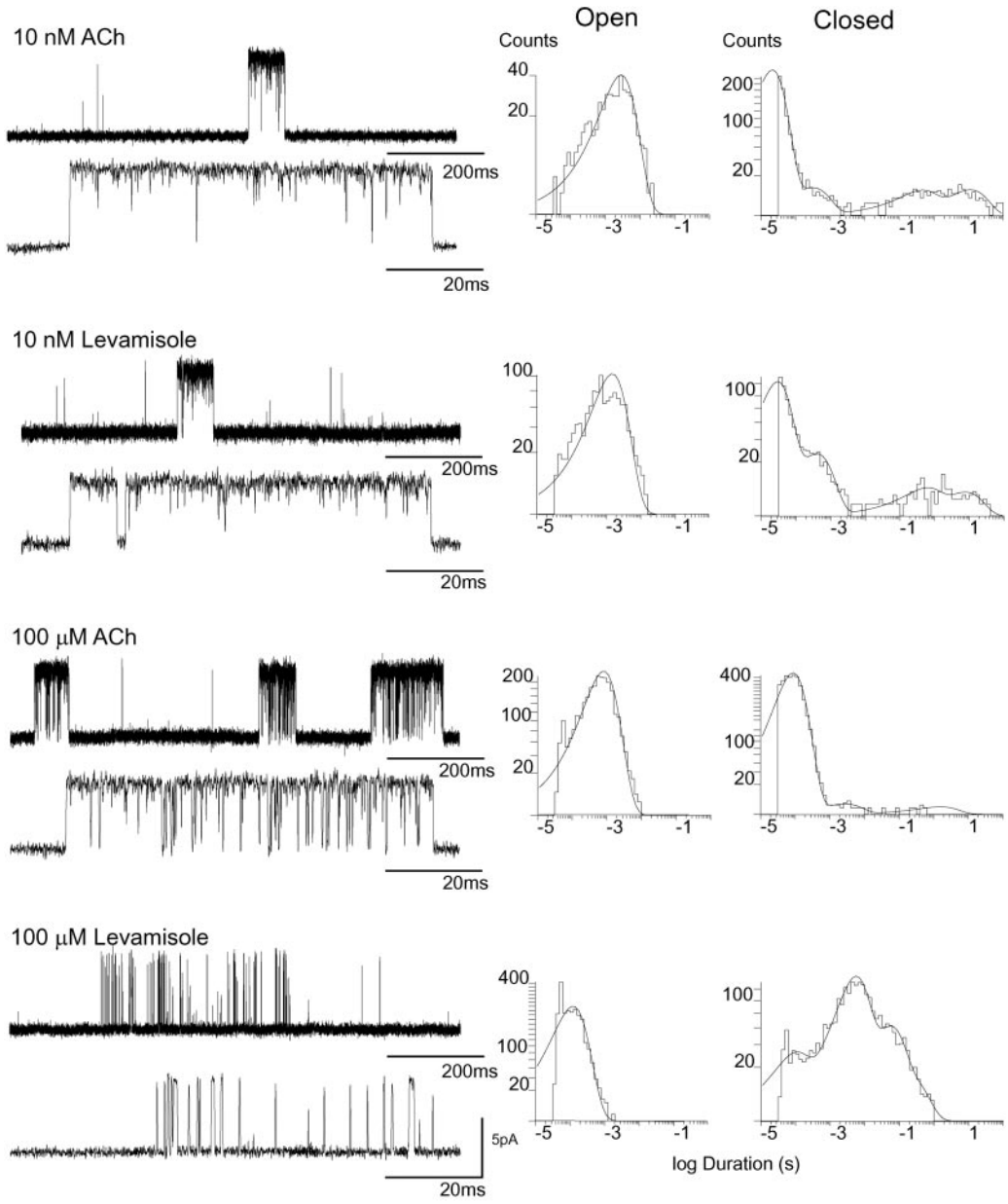

FIG. 8. **Comparison of αG153E kinetic modes.** *Left*, channel traces corresponding to AChRs containing the αG153E subunit activated by ACh and levamisole at different concentrations. Membrane potential, −70 mV. Openings are shown as upward deflections at a bandwidth of 9 kHz. *Right*, open and closed time histograms of the corresponding recordings. The clusters shown at 10 nM and 100 μM agonist correspond to the high and low P_{open} mode, respectively. The data are representative of 3–6 recordings for each condition.

potential have shown that the spastic contraction evoked by levamisole is quantitatively similar to that evoked by ACh in the muscle of *H. contortus,* which is 10–100 times more sensitive to the acute action of levamisole than the rat muscle (2).

We elucidated why mammalian muscles show lower sensitivity to the widely used anthelmintic agent levamisole than parasitic muscle, and we identified residues involved in such differential sensitivity. Our studies at the molecular level show for the first time that levamisole is a very weak agonist of mammalian muscle AChRs and reveal the basis of the low opening probability of mammalian AChR by anthelmintics, *i.e.* an extremely low efficacy for channel activation. In addition, the low efficacy of levamisole is impaired as a function of its concentration due to channel blockade. By site-directed mutagenesis we show that αGlu-153, which is conserved in all α subunits of muscle nematode, could be involved in the high efficacy of levamisole at nematode AChRs.

The weak activation process of wild-type mammalian AChRs by levamisole is revealed as follows: (i) the absence of clustering over a range of levamisole concentrations, *i.e.* AChR channels activated by levamisole, do not cluster at any concentration, whereas clear clusters of activation periods occur at ACh concentrations higher than 10 μM. In contrast, it has been shown that both ACh and levamisole activate channels in the same concentration range (1–100 μM) in nematode muscle (3). (ii) The reduced current elicited by rapid perfusion with levamisole compared with that activated by ACh. A similar result has been described for the partial agonist decamethonium, which produces a peak current of about 1% that activated by the same concentration of ACh (24). Thus, in contrast to what is observed in the nematode, kinetics of levamisole-activated mammalian AChRs greatly differ from those of AChRs activated by the natural neurotransmitter ACh.

The mutation αG153E profoundly increases the efficacy of levamisole as an agonist of mammalian AChRs. Two different gating modes can be clearly distinguished in this mutant AChR

TABLE I

Channel properties of αG153E mutant AChRs activated by ACh or levamisole

AChRs containing the αG153E mutant subunit were activated by different concentrations of levamisole or ACh. For each recording, the distributions of P_{open}, mean open duration (τ_o), and mean closed duration (τ_c) within the clusters were plotted. The data correspond to the resulting mean values and S.D. of at least four different patches for each concentration. For some conditions in which a low number of events were recorded, the data of at least three recordings were first added, and then the distributions were plotted. ND, not determined due to the absence of clustering activity.

Kinetic mode	ACh	Levamisole	τ_o	τ_c	P_{open}
	μM		ms		
HP_{open}		0.0001	1.56	0.1	0.93
		0.01	1.71 ± 0.24	0.08 ± 0.007	0.98 ± 0.009
		0.1	1.78 ± 0.05	0.07 ± 0.005	0.96 ± 0.002
		10	0.38	0.32	0.52
		50	0.26	0.32	0.45
		100	0.21	0.26	0.46
	0.01		2.40 ± 0.20	0.05 ± 0.002	0.98 ± 0.001
	1		3.20 ± 0.76	0.05 ± 0.008	0.98 ± 0.002
	10		4.30 ± 0.67	0.05 ± 0.003	0.98 ± 0.002
	50		2.70 ± 0.66	0.05 ± 0.014	0.97 ± 0.009
	100		2.80 ± 0.57	0.04 ± 0.008	0.97 ± 0.005
LP_{open}		0.01	0.43 ± 0.07	ND	ND
		1	0.31 ± 0.10	ND	ND
		10	0.23 ± 0.07	17.00 ± 6.50	0.019 ± 0.008
		50	0.19 ± 0.02	10.60 ± 1.90	0.027 ± 0.002
		100	0.16 ± 0.02	5.08 ± 0.80	0.037 ± 0.004
		300	0.08 ± 0.005	3.50 ± 1.00	0.027 ± 0.005
	1		0.9 ± 0.1	ND	ND
	10		1.1 ± 0.3	1.51 ± 0.15	0.42 ± 0.13
	50		1.1 ± 0.2	0.32 ± 0.05	0.83 ± 0.05
	100		1.2 ± 0.1	0.25 ± 0.02	0.88 ± 0.02

TABLE II

Kinetic parameters for wild-type and αG153E AChRs activated by ACh and levamisole

The data correspond to wild-type and low and high P_{open} gating modes of αG153E AChRs. Rate constants corresponding to wild-type AChRs activated by ACh (wild-type$_{ACh}$) were taken from Bouzat *et al.* (17). Values corresponding to the high P_{open} mode αG153E activated by ACh or levamisole (αG153E$_{HP\ ACh}$ and αG153E$_{HP\ Lev}$, respectively) are the result of a global fit to Scheme 3 (see "Experimental Procedures"). Constants for wild-type and low P_{open} gating mode of αG153E AChRs activated by levamisole (wild-type$_{Lev}$ and αG153E$_{LP\ Lev}$) were estimated by burst analysis of recordings at low agonist concentrations (see "Experimental Procedures"). The channel gating equilibrium constant, θ, is the ratio of the opening to closing rate constants, β/α. Data are shown as the mean ± S.D. obtained from the analysis of three different recordings for each condition. ND, not determined.

AChR	α	β	θ	k_{-2}
	s^{-1}			s^{-1}
Wild-type$_{ACh}$	1600 ± 100	50000	31	56000 ± 5000
Wild-type$_{Lev}$	5500 ± 150	400 ± 90	0.07 ± 0.009	16700 ± 1700
αG153E$_{LP\ Lev}$	7000 ± 1200	3300 ± 1300	0.47 ± 0.11	8800 ± 1200
αG153E$_{HP\ ACh}$	900 ± 100	38000 ± 4000	42 ± 3.7	ND
αG153E$_{HP\ Lev}$	730 ± 220	27000 ± 5000	37 ± 7.5	ND

on the basis of their probability of channel opening. Heterogeneous kinetics have been reported before in wild-type AChRs (25), and the number and range of kinetic modes have been shown to increase in mutant AChRs (26, 27). The analysis reveals that at concentrations low enough to avoid channel blockade, the kinetics of activation of the high P_{open} mode is almost indistinguishable for ACh or levamisole, thus supporting the effectiveness of levamisole in chemotherapy against parasites.

The mutant αG153S has been detected in patients affected by a slow-channel congenital myasthenic syndrome (22). Single channel kinetic analysis of engineered αG153S AChRs has revealed a markedly decreased rate of ACh dissociation, which causes the mutant AChR to open repeatedly during ACh occupancy (22). More recently, it has been reported that the mutation to lysine in the homologous position of the α7–5HT$_3$ subunit (G152K) conferred high affinity binding for agonists together with an increase in potency (28). Kinetic analysis of this mutant receptor suggested that the mutation affects primarily the conformational transition of activation between the closed and open channel states of the AChR (28). Our results show that the mutation to glutamic acid increases the efficacy of the agonists, but the increase is selectively higher for levamisole than for ACh. Comparison of levamisole activation between αG153S and αG153E shows that the type of amino acid at this position is also important to determine the kinetic changes.

The mechanistic bases for the kinetic changes described for the αG153E AChR may be interpreted on the basis of Scheme 4,

$$\begin{array}{ccccc} & & \overset{K_1^*}{} & & \overset{K_2^*}{} \\ R^* + A & \longleftrightarrow & AR^* + A & \longleftrightarrow & A_2R^* \\ \theta_0 \updownarrow & & \theta_1 \updownarrow & & \theta_2 \updownarrow \\ R + A & \longleftrightarrow & AR + A & \longleftrightarrow & A_2R \\ & & \underset{K_1}{} & & \underset{K_2}{} \end{array}$$

SCHEME 4

In Scheme 4, resting (R) and active (R^*) states of the receptor spontaneously interconvert in the absence of agonist, and activation is driven by progressive occupancy of the sites together with tighter binding of agonist to the active state compared with the resting state. Consistent with its physiological role, the gating reaction of diliganded AChRs is much more favorable than that of unliganded AChRs (29). From the thermodynamic principle of detailed balance, it follows that $\theta_2 = \theta_0 (K_1K_2/K_1^*K_2^*)$. This equation predicts that an increase in θ_2 may be because of the enhanced binding of agonist to the open

relative to closed state of the mutant AChR or to an effect on gating of the channel in the absence of agonist. Given that the residue 153 has been shown to be involved in agonist binding, it is probable that the mutation may affect the affinity ratio of closed and open state and that these changes are more significant for levamisole than for ACh.

The mutated amino acids form part of two different binding loops, B (αAsp-152, αGly-153, and αSer-154) and C (α-ins191), which contain residues directly contributing to the ACh binding pocket in α subunits (30, 31). Although Tyr-190, Cys-192, and Cys-193 form a barrier to entry and escape of agonist (30, 31), a proline insertion in position 191 does not introduce changes in the activation by levamisole of the AChR. This observation is consistent with the lack of effects reported previously (32) for mutations of other nearby residues. Mutations at positions 152 and 154 of α7 produced an increase in apparent binding affinity for ACh and nicotine (33). However, the most significant effects were introduced by mutations at position 153 (33).

In addition to its weaker agonist activity, levamisole acts as a more potent blocker than ACh. Hallmarks of an open channel blockade process are as follows: (i) a concentration-dependent decrease in the mean open time; (ii) a concentration-dependent increase in the fractional area of the block component; and (iii) constant mean duration of the blocked intervals across all blocker concentrations (34). These statements are confirmed at levamisole concentrations lower than 100 μM, indicating that this drug acts as an open channel blocker of mammalian AChRs. At higher concentrations, the observed blocking mechanism deviates from that of classical open channel blockers. Deviations from the linear open channel block mechanism have been also described for many noncompetitive antagonists at high concentrations (35, 36). Our findings can be explained by the fact that the blocked receptor may close, with or without trapping the blocker molecule in its site (37, 38). Another alternative explanation could be related to the presence of two or more sequential blocking sites in the pore (39, 40). In agreement with this, studies of the action of the anthelmintic morantel at the muscle AChR from *Ascaris* have suggested a complex channel blockade mechanism that could be explained by the presence of two blocking sites within the channel pore (41).

Electrophysiological studies on *Ascaris* muscle have shown that the dissociation constant of levamisole for channel block (K_B) is 123 μM at −50 mV (1). This value is similar to the one calculated for mammalian AChRs in our study. Therefore, although the activation by levamisole is strikingly different between mammalian and nematode muscle AChRs, the open channel blockade seems to be similar. This confirms that blockade is not involved in the differential selectivity of anthelmintics on both types of muscles.

Levamisole and pyrantel are believed to share the same mechanism of action although they have quite different chemical structures. Pyrantel is a tetrahydropyrimidine, whereas levamisole is an imidazothiazole. By single channel recordings, we have shown previously (42) that pyrantel acts as a low efficacious agonist and a high affinity open channel blocker of the mammalian muscle AChRs. Our results indicate that levamisole is less potent than pyrantel to activate as well as to block the mammalian AChR (42). The calculated affinity K_B for levamisole is 20-fold higher than that of pyrantel (8 μM at −70 mV). Due to the weak agonist activity of pyrantel at mammalian AChRs, it is therefore probable that its toxic effects are mediated by its blocking activity. Our results, which show that the channel-blocking ability of pyrantel is higher than levamisole, are in agreement with the reports that pyrantel has more toxic effects than levamisole (1).

Finally, resistance to the anthelmintics pyrantel and levamisole is an increasingly widespread problem in gastrointestinal nematode infestations. Assuming that our findings in the mammalian AChR can be directly extrapolated to the nematode AChR, and although this requires direct confirmation in the nematode AChR, it would be interesting to determine whether mutations at αGlu-153 are involved in the development of resistance of the parasite against anthelmintics.

Acknowledgment—We thank James Dilger for valuable discussions and comments.

REFERENCES

1. Martin, R. J., Valkanov, M. A., Dale, V. M., Robertson, A. P., and Murray, I. (1996) *Parasitology* **113,** (suppl.) S137–S156
2. Atchison, W. D., Geary, T. G., Manning, B., VandeWaa, E. A., and Thompson, D. P. (1992) *Toxicol. Appl. Pharmacol.* **112,** 133–143
3. Robertson, S. J., and Martin, R. J. (1993) *Br. J. Pharmacol.* **108,** 170–178
4. Levandoski, M. M., Piket, B., and Chang, J. (2003) *Eur. J. Pharmacol.* **471,** 9–20
5. Fleming, J. T., Squire, M. D., Barnes, T. M., Tornoe, C., Matsuda, K., Ahnn, J., Fire, A., Sulston, J. E., Barnard, E. A., Sattelle, D. B., and Lewis, J. A. (1997) *J. Neurosci.* **17,** 5843–5857
6. Richmond, J. E., and Jorgensen, E. M. (1999) *Nat. Neurosci.* **2,** 791–797
7. Wiley, L. J., Weiss, A. S., Sangster, N. C., and Li, Q. (1996) *Gene* (*Amst.*) **182,** 97–100
8. Hoekstra, R., Visser, A., Wiley, L. J., Weiss, A. S., Sangster, N. C., and Roos, M. H. (1997) *Mol. Biochem. Parasitol.* **84,** 79–187
9. Le Novère, N., and Changeux, J. P. (1999) *Nucleic Acid Res.* **27,** 340–342
10. Lewis, J. A., Wu, C. H., Levine, J. H., and Berg, H. (1980) *Neuroscience* **5,** 967–989
11. Harrow, I. D., and Gration, K. F. (1985) *Pestic. Sci.* **16,** 662–672
12. Martin, R. J., Pennington, A. J., Duittoz, A. H., Robertson, S., and Kusel, J. R. (1991) *Parasitology* **102,** 41–58
13. Bouzat, C., Bren, N., and Sine, S. (1994) *Neuron* **13,** 1395–1402
14. Bouzat, C., Roccamo, A. M., Garbus, I., and Barrantes, F. J. (1998) *Mol. Pharmacol.* **54,** 146–153
15. Hamill, O. P., Marty, A., Neher, E., Sakmann, B., and Sigworth, F. J. (1981) *Pfluegers Arch.* **391,** 85–100
16. Wang, H. L., Auerbach, A., Bren, N., Ohno, K., Engel, A. G., and Sine, S. M. (1997) *J. Gen. Physiol.* **109,** 757–766
17. Bouzat, C., Barrantes, F. J., and Sine, S. M. (2000) *J. Gen. Physiol.* **115,** 663–672
18. Bouzat, C., Gumilar, F., del Carmen Esandi, M., and Sine, S. M. (2002) *Biophys. J.* **82,** 1920–1929
19. Qin, F., Auerbach, A., and Sachs, F. (1996) *Biophys. J.* **70,** 264–280
20. Spitzmaul, G., Dilger, J. P., and Bouzat, C. (2001) *Mol. Pharmacol.* **60,** 235–243
21. Gumilar, F., Arias, H. R., Spitzmaul, G., and Bouzat, C. (2003) *Neuropharmacol.* **45,** 964–976
22. Sine, S. M., Ohno, K., Bouzat, C., Auerbach, A., Milone, M., Pruitt, J. N., and Engel, A. G. (1995) *Neuron* **15,** 229–239
23. Aceves, J., Erlij, D., and Martinez-Maranon, R. (1970) *Br. J. Pharmacol.* **38,** 602–607
24. Liu, Y., and Dilger, J. P. (1993) *Synapse* **13,** 57–62
25. Naranjo, D., and Brehm, P. (1993) *Science* **260,** 1811–1814
26. Milone, M., Wang, H. L., Ohno, K., Prince, R., Fukudome, T., Shen, X. M., Brengman, J. M., Griggs, R. C., Sine, S. M., and Engel, A. G. (1998) *Neuron* **20,** 575–588
27. Wang, H. L., Ohno, K., Milone, M., Brengman, J., Evoli, A., Batocchi, A. P., Middleton, L. T., Christodoulou, K., Engel, A. G., and Sine, S. M. (2000) *J. Gen. Physiol.* **116,** 449–460
28. Grutter, T., Prado de Carvalho, L., Le Novere, N., Corringer, P. J., Edelstein, S., and Changeux, J. P. (2003) *EMBO J.* **22,** 1990–2003
29. Engel, A. G., Ohno, K., and Sine, S. M. (2002) *Mol. Neurobiol.* **26,** 347–367
30. Brejc, K., van Dijk, W. J., Klaassen, R. V., Schuurmans, M., van Der Oost, J., Smit, A. B., and Sixma, T. K. (2001) *Nature* **411,** 269–276
31. Sine, S. M. (2002) *J. Neurobiol.* **53,** 431–446
32. Prince, R., and Sine, S. (1998) in *The Nicotinic Acetylcholine Receptor: Current Views and Future Trends* (Barrantes, F. J., ed) pp. 31–59, Springer-Verlag and R. G. Landes Co., Austin, TX
33. Corringer, P. J., Bertrand, S., Bohler, S., Edelstein, S. J., Changeux, J. P., and Bertrand, D. (1998) *J. Neurosci.* **18,** 648–657
34. Neher, E., and Steinbach, J. H. (1978) *J. Physiol.* (*Lond.*) **277,** 153–176
35. Dilger, J. P., Brett, R. S., and Lesko, L. A. (1992) *Mol. Pharmacol.* **41,** 127–133
36. Spitzmaul, G., Esandi, M. C., and Bouzat, C. (1999) *Neuroreport* **10,** 2175–2181
37. Amador, M., and Dani, J. A. (1991) *Synapse* **7,** 207–215
38. Neher, E. (1983) *J. Physiol.* (*Lond.*) **339,** 663–678
39. Dilger, J. P., Boguslavsky, R., Barann, M., Katz, T., and Vidal, A. M. (1997) *J. Gen. Physiol.* **109,** 401–414
40. Akk, G., and Steinbach, J. H. (2000) *Br. J. Pharmacol.* **130,** 249–258
41. Evans, A. M., and Martin, R. J. (1996) *Br. J. Pharmacol.* **118,** 1127–1140
42. Rayes, D., De Rosa, M. J., Spitzmaul, G., and Bouzat, C. (2001) *Neuropharmacol.* **41,** 238–245